Observation of non-linear effects in a quasi-one-dimensional antiferromagnet: magnetic excitations in $CsVCl_3$

1997 J. Phys.: Condens. Matter 9 1357

(http://iopscience.iop.org/0953-8984/9/6/019)

J. Phys.: Condens. Matter **9** (1997) 1357–1368. Printed in the UK PII: S0953-8984(97)77234-5

Observation of non-linear effects in a quasi-one-dimensional antiferromagnet: magnetic excitations in $CsVCl_3$

Toshiya Inami†§, Kazuhisa Kakurai† and Hidekazu Tanaka‡‖

† Institute for Solid State Physics, University of Tokyo, Roppongi 7-22-1, Minato-ku, Tokyo 106, Japan

‡ Department of Physics, Faculty of Science and Technology, Sophia University, Kioi-cho, Chiyoda-ku, Tokyo 102, Japan

Received 19 August 1996, in final form 5 November 1996

Abstract. The spin dynamics of the hexagonal ABX_3-type quasi-one-dimensional antiferromagnet $CsVCl_3$ is investigated by means of an inelastic neutron scattering technique. In good qualitative agreement with a recent spin-wave calculation including higher-order terms, a large scattering cross-section arising from two-magnon excitations is observed at the one-dimensional antiferromagnetic zone centre. In addition, we measured spin-wave excitations between the chains precisely and revealed that the spin-wave dispersion curves are modified in energy and in intensity on account of the anticrossing between the one-magnon branches and two-magnon continuum. These results demonstrate that anharmonic terms are important in the spin dynamics of $CsVCl_3$ even at low temperatures. We also measured the temperature dependence of the magnetic excitations and found that far above the Néel temperature the two-magnon process gives a considerable contribution to the inelastic spectrum.

1. Introduction

Quantum effects, namely, deviations from the classical linear theory, are often observed in low-dimensional magnetic systems. In a one-dimensional (1-D) $S = \frac{1}{2}$ Heisenberg antiferromagnet (AF), for instance, in strong contrast to the δ-function-like response expected for a classical system, the magnetic response corresponds to a spin-wave (SW) continuum, as confirmed in experiments on $CuCl_2{\cdot}2NC_5D_5$ [1] and $KCuF_3$ [2]. In addition, the lower boundary of the magnetic excitations is renormalized by a factor of $\pi/2$ compared with the classical case according to dCP's calculation [3].

A recent experimental study on hexagonal ABX_3-type quasi-1D AFs has revealed that low-energy excitations of these compounds are not interpreted correctly by conventional linear SW theory. Although most of the data have been discussed in connection with the Haldane gap, which is observed in a Heisenberg AF chain with integer spins, anomalous behaviour is also reported in half-integer spin systems [4]. In this paper, we report on detailed inelastic neutron scattering measurements of magnetic excitations in the hexagonal ABX_3-type quasi-1-D AF with half-integer spins $S = \frac{3}{2}$, $CsVCl_3$. We experimentally confirmed clear deviations from conventional linear SW theory for this compound and found

§ Present address: Advanced Science Research Centre, Japan Atomic Energy Research Institute, Tokai-mura, Ibaraki 319-11, Japan.

‖ Present address: Department of Physics, Faculty of Science, Tokyo Institute of Technology, Tokyo 152, Japan.

0953-8984/97/061357+12$19.50

that these results agree with a recent theoretical calculation by Ohyama and Shiba which predicts large quantum corrections to linear SW theory for a quasi-1-D helimagnet [5].

$CsVCl_3$ is a good quasi-1-D AF [6]. The magnetic ions V^{2+} are well approximated as Heisenberg spins with $S = \frac{3}{2}$ and crystallize into a simple hexagonal lattice. The magnetic chains run along the hexagonal c-axis. The intrachain AF interaction J is estimated to be -115 K from the high-temperature magnetic susceptibility [7]. The interchain AF interaction J' is supposed to be about 10^{-3}–10^{-4} of J and a weak easy-plane anisotropy D exists. Thus, the spin Hamiltonian with $S = \frac{3}{2}$ is written as

$$\mathcal{H} = -2J \sum_i \boldsymbol{S}_i \cdot \boldsymbol{S}_{i+1} - 2J' \sum_{\langle \mathrm{i,\,j} \rangle} \boldsymbol{S}_i \cdot \boldsymbol{S}_{\mathrm{j}} - D \sum_i (S_i^z)^2 \tag{1}$$

where the first sum is taken along the hexagonal c-axis and the second sum is taken in the basal plane. Below $T_N = 13.3$ K, the ordered spins align antiferromagnetically along the chain and rotate by 120° by going from one chain to the next owing to topological frustration. The directions of the ordered moments are confined to the basal plane due to the easy-plane anisotropy. To date, several inelastic neutron scattering measurements have been performed on $CsVCl_3$. Itoh *et al* measured the SW dispersion curve along the chain direction using a pulsed neutron source and found quite a steep 1-D dispersion curve that reaches 75 meV at the zone boundary [8]. The dispersion curve was well reproduced by the dispersion relation for linear SW theory: $\hbar\omega = -4J|\sin(q_c c)|$ with $J = -145$ K. Apparently, the value of $|J|$ observed in the neutron scattering measurement is larger than that obtained in the static measurement and it indicates quantum renormalization. They also reported that the variations of the intensities of the SW excitations with the momentum transfer along the c-axis are well interpreted by linear SW theory. In contrast, the magnetic excitations perpendicular to the chain axis seem to show deviations from linear SW theory [9, 10]. The low-energy magnetic excitations in $CsVCl_3$, however, have not been investigated yet in detail.

The rest of this paper is organized as follows. The linear SW approximation and results of Ohyama and Shiba's calculation are briefly introduced in the next section. Experimental procedures and results are described in section 3. Our results show a considerable two-magnon contribution to the inelastic spectra at the 1-D AF zone centre, and high-resolution measurements for the magnetic excitations perpendicular to the chain axis clearly show distorted SW dispersion curves that qualitatively agree with Ohyama and Shiba's results. The temperature evolutions of the magnetic excitations and the 1-D dispersion curves are also reported. Section 4 is devoted to discussion, and a summary is presented in section 5.

2. Theory

Ohyama and Shiba's theory is a simple extension of linear SW theory. In linear SW theory, the spin Hamiltonian is expanded in powers of $1/S$ and the terms proportional to S are treated. Ohyama and Shiba first made $1/S$ corrections to the linear theory and evaluated the SW excitation energy and neutron scattering cross-section. First we apply linear SW theory to $CsVCl_3$ and then describe Ohyama and Shiba's calculation.

In $CsVCl_3$, the ordered moments rotate by exactly 120° between the chains. In this case, the spin-wave excitation energy and neutron scattering cross-section can be obtained analytically within the linear SW approximation [11, 12].

According to the usual procedure of linear SW theory, the spin Hamiltonian (1) is expanded with respect to Fourier-transformed Bose operators $a_{\boldsymbol{q}}$ and $a_{\boldsymbol{q}}^+$, as

$$\mathcal{H} = \mathcal{H}_0 + \mathcal{H}_2 + \mathcal{H}_3 + \mathcal{H}_4 + \cdots \tag{2}$$

where $\mathcal{H}_i$ is the ith-order term of a_q and a_q^+. The first term is the Néel state energy:

$$\mathcal{H}_0 = (2J + 3J')NS^2$$

and N is the number of spins in the crystal. Owing to the equilibrium condition of the spin structure, $\mathcal{H}_1$ vanishes.

In linear SW theory, terms involving more than three raising and lowering operators, such as $\mathcal{H}_3$ and $\mathcal{H}_4$, are neglected, and only the term proportional to S, namely $\mathcal{H}_2$, is considered.

The term $\mathcal{H}_2$ is

$$\mathcal{H}_2 = (2J + 3J')NS + S\sum_q \left\{A_q(a_q^+ a_q + a_q a_q^+) - B_q(a_q a_{-q} + a_q^+ a_{-q}^+)\right\} \tag{3}$$

where

$$A_q = -2J - 3J'\left(1 + \frac{\gamma_q}{2}\right) - \frac{D}{2}$$

$$B_q = -2J\cos\pi l - \frac{9}{2}J'\gamma_q - \frac{D}{2}$$

$$\gamma_q = \frac{1}{3}\left\{\cos 2\pi h + \cos 2\pi k + \cos 2\pi(h+k)\right\}$$

$$\boldsymbol{q} = h\boldsymbol{a}^* + k\boldsymbol{b}^* + l\boldsymbol{c}^*.$$

Equation (3) is readily diagonalized by Bogoliubov transformation; then we get

$$\mathcal{H}_2 = (2J + 3J')NS + \sum_q \hbar\omega_q\left(b_q^+ b_q + \frac{1}{2}\right)$$

where b_q and b_q^+ are the annihilation and creation operators of magnons, respectively. The SW excitation energy at the wave-vector $\boldsymbol{q}$ is given by

$$\hbar\omega_q = 2S\sqrt{(A_q + B_q)(A_q - B_q)}. \tag{4}$$

The neutron scattering cross-section is also given in a simple, analytic form (see equations (6) and (7) in [13]).

The typical dispersion curves obtained parallel and perpendicular to the chain axis are depicted in figure 1(a). There are three SW branches. The polarization of one branch is along the hexagonal c- (z-) axis (the zz-mode) and the polarizations of the other branches are within the hexagonal ab-plane (xy-modes). Since the ordered moments are confined to the hexagonal basal plane in $CsVCl_3$, the zz- and xy-modes are referred to as out-of-plane and in-plane modes, respectively. As seen in the figure, the in-plane modes and the out-of-plane mode do not couple to each other. Since, at the scattering vector $\boldsymbol{q}$, one xy-mode sees the fluctuations at $\boldsymbol{q} + \boldsymbol{Q}_M$ and the other sees them at $\boldsymbol{q} - \boldsymbol{Q}_M$ in the extended Brillouin zone, where $\boldsymbol{Q}_M$ is the ordered wave vector $(\frac{1}{3}, \frac{1}{3}, 1)$, the former and the latter are referred as xy_+- and xy_--modes, respectively.

In Ohyama and Shiba's theory, higher-order terms which are neglected in the linear approximation, $\mathcal{H}_3$ and $\mathcal{H}_4$ in equation (2), are taken into consideration. For collinear spin structures, $\mathcal{H}_3$ vanishes, and $\mathcal{H}_4$, which represents interactions between spin waves, only weakly affects SW spectra as a renormalization. However, for non-collinear spin structures, such as helical or canted spin structures, $\mathcal{H}_3$ does not vanish and the second-order perturbation of $\mathcal{H}_3$ gives rise to noticeable effects on the excitation spectra [5, 14]. The origin of this quantum correction is the same as that which appeared in tetramethylammonium manganese chloride (TMMC) under a magnetic field [15]; both the cross-terms between

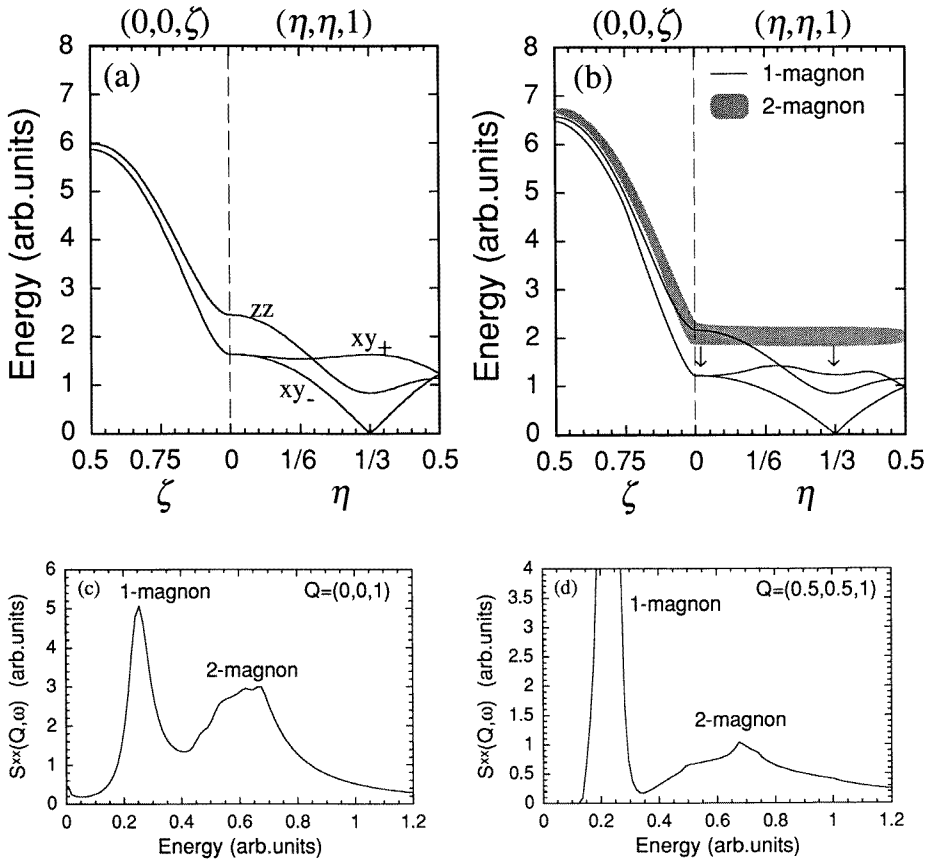

Figure 1. (a) Dispersion curves for the ABX_3-type Heisenberg AF with a planar anisotropy within the linear SW approximation. (b) An illustration of Ohyama and Shiba's calculation. Substantial two-magnon scattering appears over the entire reciprocal-lattice space. In addition, repulsion between the two-magnon band and the SW branches distorts the SW branches downward, as indicated by the arrows. (c) The in-plane component of the calculated dynamical structure factor $S^{xx}(\boldsymbol{Q}, \omega)$ at $\boldsymbol{Q} = (0, 0, 1)$. The data are quoted from [5]. (d) The in-plane component of the calculated dynamical structure factor $S^{xx}(\boldsymbol{Q}, \omega)$ at $\boldsymbol{Q} = (0.5, 0.5, 1)$. The data are quoted from [5].

conventional transverse fluctuations (one-magnon) and longitudinal fluctuations (two-magnon) arising from the non-collinear arrangement of the ordered spins, namely $\mathcal{H}_3$, and the divergence of the density of states due to one dimensionality enhance the two-magnon process [14].

The results of Ohyama and Shiba's calculations are summarized pictorially in figure 1(b) for the sake of comparison with the linear SW calculation, figure 1(a). The in-plane components of the calculated dynamical structure factor $S^{xx}(\boldsymbol{Q}, \omega)$ at $\boldsymbol{Q} = (0, 0, 1)$ and $(0.5, 0.5, 1)$ are also shown in figures 1(c) and 1(d) as functions of the excitation energy. The important differences between the linear theory and their calculations are the following two points.

(A) Throughout the whole reciprocal-lattice space, especially at the 1-D AF zone centre $\boldsymbol{Q} = (\eta, \eta, 1)$, a band-like cross-section due to two-magnon processes exists in addition to

conventional SW (one-magnon) excitations at $T = 0$ K. These two-magnon scatterings are seen in figures 1(c) and 1(d) as broad peaks at around $E = 0.6$ arbitrary units. When S is sufficiently small or the one dimensionality is good enough, the intensities of the two-magnon scatterings can be of comparable magnitude to the one-magnon scattering, as shown in figure 1(c).

(B) Due to the one-magnon–two-magnon interactions, SW spectra are modified in both excitation energy and scattering intensity, particularly at the 1-D AF zone centre $\boldsymbol{Q} = (\eta, \eta, 1)$. The interacting terms also give rise to a finite lifetime for SW excitations; hence certain SW peaks show a finite linewidth at $T = 0$ K.

3. Experimental results

Inelastic neutron scattering experiments were performed on the ISSP triple-axis spectrometers PONTA and HER installed at the research reactor JRR-3M at the Japan Atomic Energy Research Institute (JAERI), Tokai. Most of the data from PONTA were taken with the final energy fixed at 14.7 meV and with the two sets of collimations 15′–20′–40′–40′ and 40′–40′–40′–40′. The fixed final energy 30.5 meV and the collimation 40′–40′–40′–40′ were used to measure the magnetic excitations along the chain direction. For the high-resolution measurements made on HER, cold neutrons with fixed initial energy 6.35 meV and the collimation beyond the monochromator 40′–80′–80′ were employed. A vertically bent pyrolytic graphite monochromator and analyser were used in all cases. To reduce higher-order contaminations a pyrolytic graphite filter was used on PONTA. A cylinder-shaped single crystal, the volume of which is about 1.5 cm^3, was placed in an ILL-type orange cryostat with the [110] and [001] axes in the scattering plane so as to make measurements in the $(\eta\eta\zeta)$ plane. Closed-cycle ^{4}He refrigerators were also used for the measurements of the $\boldsymbol{Q}$-dependence along the chain direction and the temperature dependence.

We first present the major features of the magnetic excitations at the 1-D AF zone centre at $T = 1.6$ K. Constant-$\boldsymbol{Q}$ scans were measured at several scattering vectors $\boldsymbol{Q} = (\eta, \eta, 1)$ using thermal neutrons on PONTA. Typical inelastic profiles are shown in figure 2. The most prominent result was obtained at $\boldsymbol{Q} = (0, 0, 1)$. As shown in figure 1(a), at $\boldsymbol{Q} = (0, 0, 1)$ linear SW theory predicts one out-of-plane mode and two degenerate in-plane modes. Since neutron magnetic scattering only 'sees' fluctuations perpendicular to the scattering vector, the out-of-plane mode—which is the fluctuations along the c-axis—cannot be observed at $\boldsymbol{Q} = (0, 0, 1)$; within the linear SW approximation only one SW peak should be observed. As seen in figure 2(a), however, at $\boldsymbol{Q} = (0, 0, 1)$ a broad peak at around 6 meV is observed in addition to a sharp peak at 2.6 meV. The lower peak can be attributed to the two degenerate xy-polarized SW branches. At $\boldsymbol{Q} = (0, 0, 3)$, a position equivalent to $(0, 0, 1)$, the intensity of the broad peak is reduced almost in proportion to the square of the magnetic form factor of V^{2+} ions [16]. Hence the broad peak is of magnetic origin. The solid line in figure 2(a) was obtained from a least-squares fit in which we took into account the instrumental resolution and SW dispersion; a sharp peak and a broad one are considered. The contribution of the sharp peak is depicted by the broken line and the line shape is limited by the instrumental resolution. The asymmetric line shape is due to the steep 1-D dispersion. From this fit, the integrated intensity of the broad peak is estimated to be about five times larger than that of the sharp peak. This broad peak changes its line shape to a much broader one when going along the [110] direction. A constant-$\boldsymbol{Q}$ scan at $\boldsymbol{Q} = (-0.5, -0.5, 1)$ is shown in figure 2(b). Three almost degenerate SW branches are expected at $\boldsymbol{Q} = (-0.5, -0.5, 1)$. We show a single sharp peak convoluted with a resolution function by the broken line. The shaded area thus shows additional intensity and it is extremely broad.

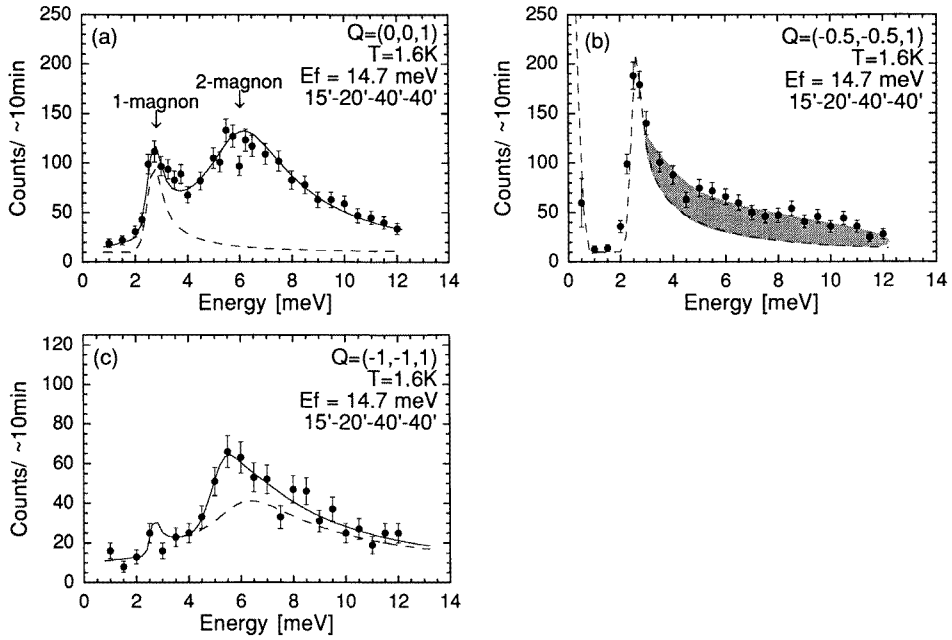

Figure 2. Typical inelastic profiles in $CsVCl_3$ measured at three different values of $\boldsymbol{Q}$. (a) At $\boldsymbol{Q} = (0, 0, 1)$. The solid line corresponds to two peaks convoluted with the instrumental resolution function. In addition to a sharp one-magnon peak at 2.6 meV, depicted by the broken line, a large, broad peak of the two-magnon band at around 6 meV is observed. (b) At $\boldsymbol{Q} = (-0.5, -0.5, 1)$. The broken line represents a single sharp peak convoluted with the instrumental resolution. The extra intensity indicated as the shaded area is expected to be the two-magnon scattering. (c) At $\boldsymbol{Q} = (-1, -1, 1)$. The solid line is the total intensity and broken line represents the contribution of in-plane fluctuations. The out-of-plane mode is observed.

Here we should recall that a broad two-magnon continuum is expected along $\boldsymbol{Q} = (\eta, \eta, 1)$ from Ohyama and Shiba's calculation. Although the parameters used for the calculation are different from those for $CsVCl_3$, a qualitative comparison between the theory and experiments is possible. For $\boldsymbol{Q} = (0, 0, 1)$, because figure 2(a) displays an in-plane component of the scattering cross-section and figure 1(c) shows the in-plane component of the dynamical structure factor, the two figures can be compared directly with each other, and one can see that the experimentally observed inelastic profiles closely resemble the calculated inelastic spectrum. For $\boldsymbol{Q} = (0.5, 0.5, 1)$, the theory predicts an extremely broad two-magnon continuum (figure 1(d)). This feature also seems to agree with the observation. Such an accordance between the experiment and theory strongly suggests that the broad scattering originates from a non-linear effect, i.e., it can be attributed as two-magnon scattering.

In figure 2(c), the inelastic spectrum at $\boldsymbol{Q} = (-1, -1, 1)$ is shown. At $\boldsymbol{Q} = (-1, -1, 1)$, another position equivalent to $(0, 0, 1)$, the out-of-plane mode can be seen in addition to the excitations with in-plane fluctuations observed at $\boldsymbol{Q} = (0, 0, 1)$; three peaks, i.e., two SW peaks and a broad peak, should be observed. Since it is difficult to divide the data into three peaks directly by a least-squares fit, we first estimated the contribution of in-plane fluctuations using the data measured at $\boldsymbol{Q} = (0, 0, 1)$ and it is shown by the broken line in the figure. The absorption, instrumental resolution, magnetic form factor and polarization

are taken into account. Then we fitted the rest of the intensity with a single peak. The solid line in the figure is the total intensity. It can be seen that the out-of-plane mode exists at $\boldsymbol{Q} = (-1, -1, 1)$, as expected.

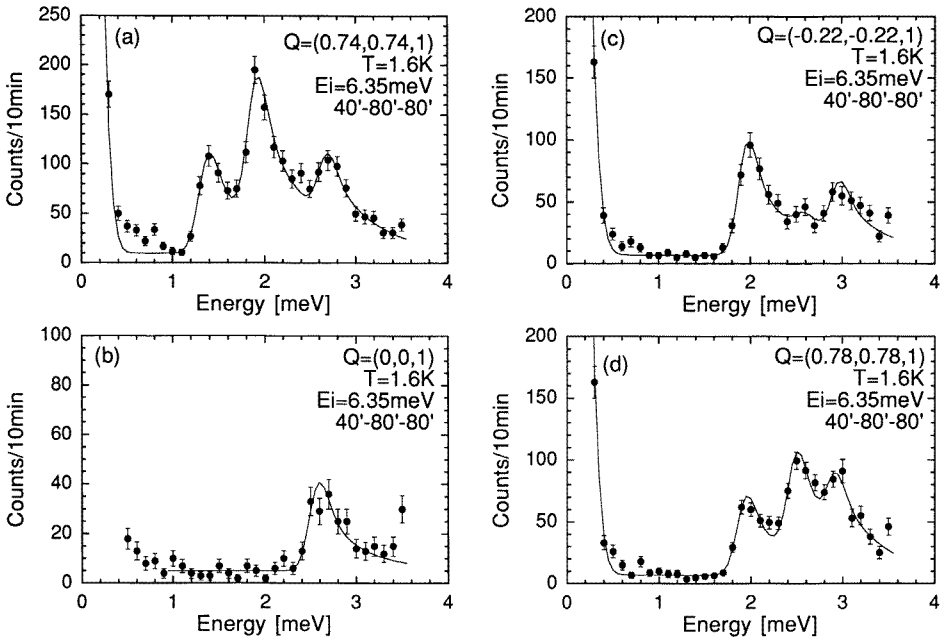

Figure 3. Typical inelastic spectra for $CsVCl_3$ measured on HER at 1.6 K. Solid lines indicate least-squares fits, taking into account the instrumental resolution function and spin-wave dispersion.

To determine the SW dispersion curves perpendicular to the chain axis in detail, we used cold neutrons on HER. In figure 3, several constant-$\boldsymbol{Q}$ scans are shown. The solid lines are least-squares fits in which the instrumental resolution function and SW dispersion are considered. Again, the asymmetric line shape is due to the steep 1-D dispersion. A finite linewidth is necessary to get a reasonably good fit, and a constant linewidth of 0.2 meV (FWHM) was used for all of the excitations shown in figure 3. Since the small resolution volume facilitates discriminating each excitation, all of the three SW branches that are expected in $CsVCl_3$ were clearly observed. The excitation energies of the SW peaks were extracted from the fits and are summarized in figure 4. All points except those on the *zz*-branch at $\boldsymbol{Q} = (0, 0, 1)$ are obtained from the cold-neutron experiments. The solid lines are guides to the eye and the broken lines are dispersion curves calculated from linear SW theory, where $J = -145$ K [8], $J' = -0.08$ K† and $D = -0.045$ K are used. The polarization of the SW branches was identified by comparing the intensities at equivalent positions for several reciprocal-lattice points, making use of the fact that the neutron magnetic scattering intensity depends on the relative directions of the scattering vector and the polarization of

† A conventional way to estimate the interchain coupling J' is to fit interchain dispersion curves within the linear SW approximation. For $CsVCl_3$, however, since the dispersion curves deviate from those expected from linear SW theory, as observed, it is impossible to extract exact J' from a fit in principle. We chose $J' = -0.08$ K so as to fit the gapless branch near $\boldsymbol{Q} = (\frac{1}{3}, \frac{1}{3}, 1)$, because lower-energy excitations are expected to be less affected by two-magnon processes; hence we stress that this value is only a lower bound for $|J'|$.

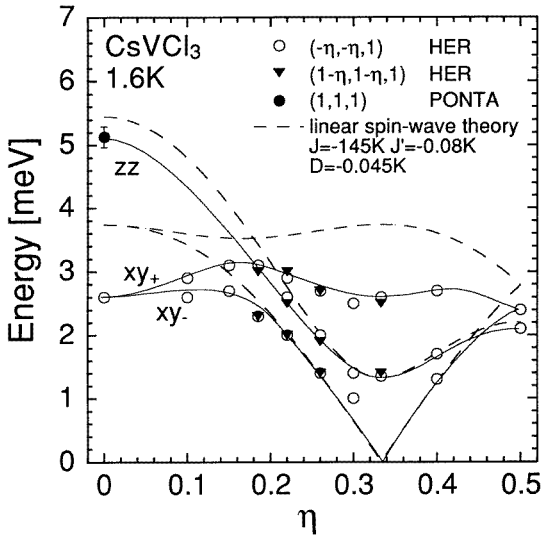

Figure 4. Observed SW dispersion curves of $CsVCl_3$ at 1.6 K. Full lines are only guides to the eye. Note that the xy_+-branch has minima at $\boldsymbol{Q} = (0, 0, 1)$ and $(\frac{1}{3}, \frac{1}{3}, 1)$ in contrast to the SW dispersion curve calculated within the linear SW approximation (broken lines).

the fluctuations. For instance, as seen in figures 3(c) and 3(d), an excitation peak at 2.5 meV is weaker than the other two peaks at $\boldsymbol{Q} = (-0.22, -0.22, 1)$, but stronger then those at $\boldsymbol{Q} = (0.78, 0.78, 1)$. This indicates that the excitation mode at 2.5 meV is accompanied with zz-fluctuations (the out-of-plane mode). The crucial difference between the experimental results and SW dispersion curves deduced from linear SW theory is that the SW branch designated as xy_+ in figure 4 shows minima in energy at $\boldsymbol{Q} = (0, 0, 1)$ and $(\frac{1}{3}, \frac{1}{3}, 1)$—that is, at the zone centre. This result is in good accordance with Ohyama and Shiba's theory. As described in section 2, they predicted that due to anticrossing between one- and two-magnon excitations, one-magnon branches are strongly renormalized, especially at the zone centre (figure 1(b)). Therefore our results definitely illustrate that considerable two-magnon–one-magnon interactions do exist in $CsVCl_3$.

The magnetic excitations along the 1-D direction were measured in the constant-E mode at energy transfers of 20, 30 and 35 meV at $T = 5.1$ K. In figure 5, a typical result is shown. The solid line in the figure is a least-squares fit in which the instrumental resolution and dispersion curves of the excitations are taken into account. This fit to the classical 1-D AF dispersion curve $\hbar\omega = -4J|\sin(\pi\zeta)|$ gives the intrachain interaction $J = -149 \pm 2$ K, which is in agreement with the value obtained by Itoh *et al* ($J = -145 \pm 1$ K) [8]. The dependence of the integrated intensity on the momentum transfer along the chain axis also follows well the expectations of linear SW theory. The line shape of all three scans was well reproduced by a Lorentzian of linewidth about 6 meV (FWHM). All of the results obtained at these large energy transfers essentially agree with a recent study made using a pulsed neutron source [8].

The temperature dependences of the magnetic excitations were measured mainly at $\boldsymbol{Q} = (0, 0, 1)$ on PONTA using thermal neutrons. As shown in figure 6, somewhat below T_N the one-magnon peak at 2.6 meV observed at $T = 1.6$ K is already heavily overdamped and seems to contribute to the low-energy ($E \leqslant 2$ meV) scattering, while the two-magnon peak remains unchanged. At $T = 40$ K, nearly $3T_N$, the two-magnon peak still persists

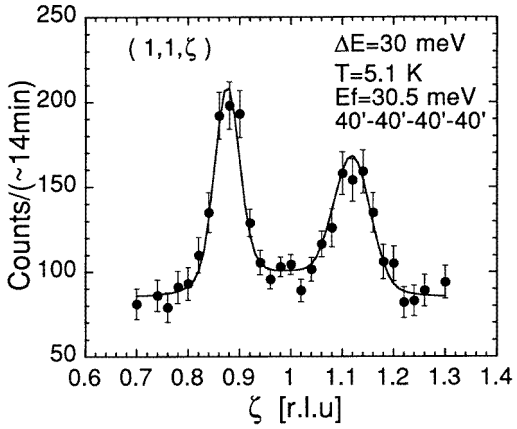

Figure 5. A constant-E scan measured at the energy transfer 30 meV. The solid line is a least-squares fit.

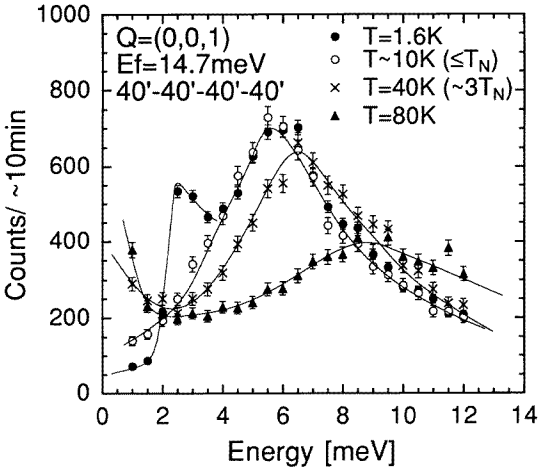

Figure 6. The temperature evolution of the magnetic excitations in $CsVCl_3$ at $\boldsymbol{Q} = (0, 0, 1)$. The solid lines are only guides to the eye. The broad peak of the two-magnon continuum does not broaden out at $T = 40$ K ($3T_N$) and can be observed even at $T = 80$ K.

with almost the same shape as at $T = 1.6$ K, and quasi-elastic scattering (below 1 meV) appears. As the temperature is increased, the two-magnon peak slowly loses intensity with its peak position moving towards the higher energy, and the quasi-elastic scattering increases further. At $T = 150$ K, the two-magnon peak could not be observed in the energy region for which we made measurements. The temperature evolution of the magnetic excitations for other momentum transfer vectors at the 1-D AF zone centre seems to show very similar behaviour. In these coarse-resolution measurements, at $T = 20$ K the inelastic profiles are similar to those in the ordered phase, and broadened low-temperature SW excitations can be observed. Above $T = 40$ K, at $\boldsymbol{Q} = (-0.2, -0.2, 1)$, the magnetic excitations seem to be almost the same as those at $\boldsymbol{Q} = (0, 0, 1)$ and only broad two-magnon scattering was observed.

4. Discussion

As we have seen in the previous section, Ohyama and Shiba's calculation explains well the noticeable features of the magnetic excitations in $CsVCl_3$. In this section, we further compare our results with their calculation in terms of the linewidth and intensity of the SW excitations. Then later we discuss the temperature dependence of the magnetic excitations at the 1-D AF zone centre.

Owing to interaction terms connecting one- and two-magnon excitations, conventional SW excitations have finite lifetimes even at $T = 0$ K and, consequently, show finite linewidth. Indeed, as mentioned in the previous section, if one assumed a narrow enough linewidth for each SW peak, fitting curves would deviate systematically from the observed data. Since it is hard to extract a precise value of the linewidth directly from a least-squares fit because of the rather poor statistics, we used the constant linewidth of 0.2 meV (FWHM) for every SW peak except for the *zz*-branch at $\boldsymbol{Q} = (-1, -1, 1)$ and obtained reasonably good fits. Thermal fluctuations may give rise to finite lifetimes for SW excitations. We measured the peak intensity of the magnetic Bragg reflection $(\frac{1}{3}\frac{1}{3}1)$ and found it almost constant below $T = 4$ K; thus it is thought that thermal fluctuations are negligible at the measured temperature 1.6 K. Accordingly, the observed linewidth can be attributed to a quantum origin, and supports Ohyama and Shiba's results. For the *zz*-branch at $\boldsymbol{Q} = (-1, -1, 1)$, we required a broader linewidth of 0.6 meV (FWHM) to fit the data. Ohyama and Shiba expected a relatively broad linewidth for this peak; thus this is also consistent.

For the magnetic excitations at high energy transfers, we found a linewidth of about 6 meV. Itoh *et al* also observed almost the same linewidth and pointed out that this linewidth is clearly larger than the expectation from the classical theory [8]. The two-magnon continuum might contribute to it. Along the 1-D dispersion curve, as shown in figure 1(b), the two-magnon band is expected to have a dispersion curve parallel to the conventional SW branches [17]. In $CsVCl_3$, the scattering cross-section of the two-magnon process is expected to be quite a lot weaker than that of SW excitations at high-energy transfers; thus a tail due to a two-magnon continuum might be observed on the high-energy side of the SW excitations. High-resolution measurements are required to clarify this point.

Because this compound has a large absorption cross-section for neutrons, the integrated intensities of the SW peaks at different crystal orientations (i.e. different $\boldsymbol{Q}$) cannot be unambiguously related. Hence, here we compare the experimental results with the theory only qualitatively. According to Ohyama and Shiba, notable deviations from linear SW theory are observed as weak *xy*-branches at around $\boldsymbol{Q} = (0, 0, 1)$ and a strong xy_+-branch at around $\boldsymbol{Q} = (\frac{1}{3}, \frac{1}{3}, 1)$ (figure 4 in [5]). The experimental results seem to have a similar tendency. After performing corrections for the absorption and magnetic form factor [16], we normalized the observed intensities of the SW excitations on the *zz*-branch. Although there are still ambiguities, it is safe to say that the observed intensity of the *xy*-branches at $\boldsymbol{Q} = (0, 0, 1)$ is considerably (about three times) weaker than expected from linear SW theory. The intensity of the xy_+-branch at around $\boldsymbol{Q} = (\frac{1}{3}, \frac{1}{3}, 1)$ also appears to be stronger than that calculated from linear SW theory. On the whole, we may conclude that the magnetic excitations of $CsVCl_3$ agree well with Ohyama and Shiba's calculation as regards intensity also.

Near and above T_N, we observed the two-magnon peak at the 1-D AF zone centre as shown in figure 6. Near T_N, the one-magnon excitation observed at the lowest temperature is damped because of the lack of long-range order, while the two-magnon peak remains almost unchanged. It is usually expected that two-magnon excitations are also damped

when the one-magnon excitations that compose the two-magnon excitations are damped; thus this seems to imply that the two-magnon excitations exist in spite of the disappearance of the original one-magnon excitations. In addition, the mostly inelastic spectrum at the 1-D AF zone centre far above T_N seems even to be inconsistent with the conventional view of magnetic excitations in the 1-D short-range-ordered phase. Usually, magnetic excitations in the 1-D short-range-ordered region exhibit well-defined SW excitations at wavelengths less than the correlation range, but show quasi-elastic scattering being governed by a diffusion process near the 1-D AF zone centre (for small q_c). Out-of-plane modes at the 1-D AF zone centre may exist above T_N in a planar system if the anisotropy gap $S^2\sqrt{4JD}$ exceeds the ambient temperature k_BT [15], but only in-plane fluctuations contribute to the broad peak observed at $\boldsymbol{Q} = (0, 0, 1)$; thus this is not the case. As a result, our data indicate that long-wavelength 1-D fluctuations in $CsVCl_3$ consist of a finite-energy component as well as a quasi-elastic component. It is emphasized that the same phenomena were observed for other ABX_3-type AFs with half-integer spins, $CsMnBr_3$ and $CsMnI_3$. In $CsMnBr_3$, at low temperatures a broad two-magnon peak at $\boldsymbol{Q} = (0, 0, 1)$ gives only a very weak scattering intensity, but this grows with increasing temperature and considerable intensity remains up to about $3T_N$ [13, 18]. Above T_N, $CsMnI_3$ also shows a broad peak at the 1-D AF zone centre [18]. Therefore the observed finite-energy excitations at small q_c seem to be common in hexagonal ABX_3-type AFs with half-integer spins. We thus propose that these finite-energy excitations at the 1-D AF zone centre above T_N originate from the two-magnon process enhanced by a helical arrangement of the spins. We believe that, though there is no well-defined one-magnon excitation at $q_c = 0$ due to the finite correlation length, the remaining short-range order among the chains may be enough to cause the local helical arrangement to be retained and to enhance the two-magnon process.

5. Summary

The magnetic excitations in $CsVCl_3$ were measured by means of inelastic neutron scattering. Large contributions of the two-magnon process were observed at the 1-D AF zone centre $\boldsymbol{Q} = (\eta, \eta, 1)$ together with the conventional SW excitations. The detailed measurements along $\boldsymbol{Q} = (\eta, \eta, 1)$ showed for the first time precise SW dispersion curves perpendicular to the chain axis in this compound, and revealed that the observed SW dispersion is considerably distorted compared with the expectation from the linear SW theory. These results are in good qualitative agreement with the SW theory including higher-order non-linear terms and provide strong experimental evidence that the multi-magnon process plays an important role in the spin dynamics in $CsVCl_3$ at low temperatures. In the one-dimensionally short-range-ordered region, the two-magnon peak was observed at the 1-D AF zone centre. It seems that the non-linear process is indispensable for a full understanding of the spin dynamics in ABX_3-type antiferromagnets with half-integer spins at high temperatures.

Acknowledgments

We would like to thank Dr T Ohyama for providing the data from his calculation. We are grateful for helpful discussions with Drs T Ohyama, S Itoh, M Enderle and D Welz, and Professor S E Nagler.

References

[1] Heilmann I U, Shirane G, Endoh Y, Birgeneau R J and Holt S L 1978 *Phys. Rev.* B **18** 3530
[2] Nagler S E, Tennant D A, Cowley R A, Perring T G and Satija S K 1991 *Phys. Rev.* B **44** 12 361
Tennant D A, Perring T G, Cowley R A and Nagler S E 1993 *Phys. Rev. Lett.* **70** 4003
[3] des Cloizeaux J and Pearson J J 1962 *Phys. Rev.* **128** 2131
[4] Kakurai K 1992 *Physica* B **180+181** 153
[5] Ohyama T and Shiba H 1993 *J. Phys. Soc. Japan* **62** 3277
[6] Hirakawa K, Ikeda H, Kadowaki H and Ubukoshi K 1983 *J. Phys. Soc. Japan* **52** 2882
[7] Niel Y M, Cros C, Pouchard M and Chaminade J P 1977 *J. Solid State Chem.* **20** 1
[8] Itoh S, Endoh Y, Kakurai K and Tanaka H 1995 *Phys. Rev. Lett.* **74** 2375
[9] Feile R, Kjems J K, Hauser A, Güdel H U, Falk U and Furrer A 1984 *Solid State Commun.* **50** 435
[10] Kadowaki H, Ubukoshi K, Hirakawa K, Belanger D P, Yoshizawa H and Shirane G 1986 *J. Phys. Soc. Japan* **55** 2846
[11] Yoshida K and Miwa H 1961 *J. Appl. Phys.* **32** 8S
[12] Kadowaki H, Ubukoshi K and Hirakawa K 1983 *J. Phys. Soc. Japan* **52** 1799
[13] Falk U, Furrer A, Güdel H U and Kjems J K 1987 *Phys. Rev.* B **35** 4888
[14] Osano K, Shiba H and Endoh Y 1982 *Prog. Theor. Phys.* **67** 995
[15] Heilmann I U, Kjems J K, Endoh Y, Reiter G F, Shirane G and Birgeneau R J 1981 *Phys. Rev.* B **24** 3939
[16] Watson R E and Freeman A J 1969 *Acta Crystallogr.* **14** 27
[17] Ohyama T, private communication
[18] Inami T *Thesis* University of Tokyo